

is stable and does not backreact and thus the production of electricity is not restricted to only the illumination period.

A concluding remark relates to the light-induced reduction of nitrate in a biological environment. It is well-known that photosynthetic organisms, in particular, higher plants, can use nitrate instead of carbon dioxide as an electron acceptor. These organisms reduce nitrate to ammonia with chlorophyll as the sensitizer. The present system accomplishes a first step in mimicking this important photobiological reaction.

Acknowledgment. A.J.F. acknowledges support by the Office of Basic Energy Sciences, Division of Chemical Energy, U.S. Department of Energy (Contract EG-77-C-01-4042); M.G. is grateful for support by the Swiss National Foundation and Ciba-Geigy, Switzerland.

Registry No. Nitrate, 14797-55-8; water, 7732-18-5; ethanol, 64-17-5; *N*-methylphenothiazine, 1207-72-3; *N,N,N',N'*-tetramethylbenzidine, 366-29-0; nitrite, 14797-65-0; NaLS, 151-21-3; DTAC, 112-00-5.

Contribution from the Laboratory of Inorganic Chemistry, College of General Education, and Department of Chemistry, Faculty of Science, Nagoya University, Nagoya 464, Japan, and Institute for Molecular Science, Myodaiji, Okazaki 444, Japan

Ab Initio MO Calculations for Hexacyano Complexes

MITSURU SANO,*^{1a} HIROSHI KASHIWAGI,^{1b} and HIDEO YAMATERA^{1c}

Received March 12, 1982

Ab initio LCAO SCF MO calculations were carried out on the hexacyano complexes $[M(CN)_6]^{3-}$ ($M = Cr, Mn, Fe,$ and Co) and $[Fe(CN)_6]^{4-}$. The core orbital energies and valence shell ionization potentials are discussed in comparison with XPS results. The maps of the electron-density changes in the formation of coordination bonds are presented. These maps indicate σ donation and π back-donation that are greater in the cobalt(III) than in the chromium(III) complex. A more extensive back-donation is seen in the iron(II) complex. The mechanisms of these interactions are elucidated.

Introduction

Cyanide complex salts have long been known as typical coordination compounds of transition-metal ions having various symmetries, O_h , D_{4h} , T_d , and D_{3h} . The complexes have been the subject of extensive experimental studies in relation to the electronic structures in the ground and excited states.^{2a}

In particular, octahedral complexes are of fundamental importance in the investigations of the coordination chemistry. The absorption spectra of these complexes have been reported by Alexander and Gray.^{2b} They discussed the changes of the relative energies of the metal and ligand orbitals and pointed out the importance of the back-donation on the basis of charge-transfer spectra. Jones³ and Griffith et al.⁴ have reported the force constants of metal-carbon and carbon-nitrogen bonds and discussed the natures of the σ and π bondings. The X-ray photoelectron spectra (XPS) have been studied to investigate directly the valence orbital levels of the cyanide complexes by Calabrese et al.,⁵ Prins et al.,⁶ and Vannerberg.⁷ Vannerberg⁷ and Sano et al.⁸ have reported XPS studies on the core binding energies of cyano ligands and discussed the relation between their shifts and the change in the charge distribution throughout a series of cyano complexes.

On the other hand, theoretical approaches to the electronic structure of the octahedral cyanide complexes have been

carried out in terms of the Wolfsberg-Helmholz method by Kida et al.⁹ and Alexander and Gray^{2b} and the MS-X α method by Larsson et al.^{10,11} The iron cyanide complexes were also studied in terms of the CNDO method¹² and the MS-X α method.^{13,14}

Alexander and Gray^{2b} have shown many important aspects of the electronic structures of cyano complexes. However, the detailed electronic structure, orbital interaction, charge distribution, etc. are not shown. Larsson¹¹ has studied the atomic charges of cyano complexes and showed the extent of σ donation and π back-donation.

We have already reported the electronic structure of $[Co(CN)_6]^{3-}$ obtained by the Hartree-Fock method.¹⁵ In previous papers, we used electron density maps to demonstrate σ donation and π back-donation occurring on the coordination of cyanide ions to a cobalt ion and to show a significant relaxation on the ionization of a d electron. The mechanism of coordinate-bond formation was discussed in terms of interactions between the metal and ligand orbitals. Furthermore, we have also reported the DV-X α MO calculations of a series of hexacyano complexes, $[M(CN)_6]^{3-}$ ($M = Cr, Mn, Fe,$ and Co) and $[Fe(CN)_6]^{4-}$.¹⁶

- (1) (a) Laboratory of Inorganic Chemistry, Nagoya University. (b) Department of Chemistry, Nagoya University. (c) Institute for Molecular Science.
- (2) (a) A. G. Sharpe, "The Chemistry of Cyano Complexes of the Transition Metals", Academic Press, London, 1976. (b) J. J. Alexander and H. B. Gray, *J. Am. Chem. Soc.*, **90**, 4260 (1968).
- (3) L. H. Jones and B. I. Swanson, *Acc. Chem. Res.*, **9**, 128 (1976).
- (4) W. P. Griffith and G. T. Turner, *J. Chem. Soc.*, 858 (1970).
- (5) A. Calabrese and R. G. Hayes, *J. Am. Chem. Soc.*, **96**, 5054 (1974).
- (6) R. Prins and P. Biloen, *Chem. Phys. Lett.*, **30**, 340 (1975).
- (7) N. G. Vannerberg, *Chem. Scr.*, **9**, 122 (1976).
- (8) M. Sano and H. Yamatera, *Bull. Chem. Soc. Jpn.*, **54**, 2023 (1981).

- (9) S. Kida, K. Nakamoto, J. Fujita, and R. Tsuchida, *Bull. Chem. Soc. Jpn.*, **31**, 7 (1958).
- (10) S. Larsson and M. Lopes De Siqueira, *Chem. Phys. Lett.*, **44**, 537 (1976).
- (11) S. Larsson, *Theor. Chim. Acta*, **49**, 45 (1978).
- (12) D. W. Clack and M. Monshi, *Mol. Phys.*, **31**, 1607 (1976).
- (13) D. Guenzburger, B. Maffeo, and S. Larsson, *Int. J. Quantum Chem.*, **12**, 383 (1977); D. Guenzburger, B. Maffeo, and M. L. De Siqueira, *ibid.*, **38**, 35 (1977).
- (14) A. Aizman and D. A. Case, *Inorg. Chem.*, **20**, 528 (1981).
- (15) M. Sano, Y. Hatano, and H. Yamatera, *Chem. Phys. Lett.*, **60**, 257 (1979); M. Sano, Y. Hatano, H. Kashiwagi, and H. Yamatera, *Bull. Chem. Soc. Jpn.*, **54**, 1523 (1981).
- (16) M. Sano, H. Adachi, and H. Yamatera, *Bull. Chem. Soc. Jpn.*, **54**, 2881 (1981).

Table I. Core Orbital Energies by ab Initio MO, DV- $X\alpha$ MO, and XPS Results (eV)

	Cr ³⁺	Mn ³⁺	Fe ³⁺	Co ³⁺	Fe ²⁺
Ab Initio					
N 1s	412.6	412.5	412.4	412.4	407.8
C 1s	295.1	295.1	295.0	295.1	290.6
$\Delta E(N\ 1s-C\ 1s)$	117.5	117.4	117.4	117.3	117.2
DV- $X\alpha$					
$\Delta E(N\ 1s-C\ 1s)$	110.0	109.9	109.9	109.6	109.8
XPS					
$\Delta E(N\ 1s-C\ 1s)$	113.6	113.4	113.3	113.2	113.1
Ab Initio					
Fe 2p			737.6		728.4
$\Delta E(Fe\ 2p-N\ 1s)$			325.2		320.6
$\Delta E(Fe\ 2p-C\ 1s)$			442.6		437.8
XPS					
$\Delta E(Fe\ 2p-N\ 1s)$			312.4		311.1
$\Delta E(Fe\ 2p-C\ 1s)$			425.7		424.2

In the present study, ab initio MO computations of these cyano complexes have been undertaken in order to investigate (1) the relationship between the calculated orbital energies and the ionization potentials for core and valence electrons, (2) the bonding structures, and (3) the electron-density changes occurring on the formation of coordinate bonds in the series of metal cyanide complexes.

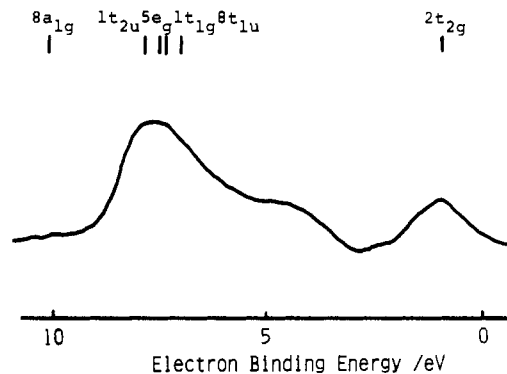
Computational Method

The present calculation is of the LCAO MO SCF type, using a basis set of Gaussian functions. The basis sets for metals were chosen as follows. The primitive GTF (Gaussian-type function) sets, [12s, 6p, 4d], given by Roos¹⁷ were modified by replacing the two most diffuse s functions (11th and 12th) by one s and one p function, each of which has an exponent 0.45 times as large as that of the tenth s function. The resulting [11s, 7p, 4d] functions were contracted to [7s, 5p, 2d]. For C and N, [9s, 5p] sets¹⁸ were contracted to [4s, 2p] sets. Thus, 340 GTF's were contracted to 152 GTO's (Gaussian-type orbitals). The ions were assumed to be octahedral and the inter-atomic distance were taken as follows:¹⁹ Cr-C = 2.077 and C-N = 1.136 Å for [Cr(CN)₆]³⁻; Mn-C = 2.002 and C-N = 1.142 Å for [Mn(CN)₆]³⁻; Fe-C = 1.950 and C-N = 1.143 Å for [Fe(CN)₆]³⁻; Co-C = 1.896 and C-N = 1.154 Å for [Co(CN)₆]³⁻; Fe-C = 1.925 and C-N = 1.167 Å for [Fe(CN)₆]⁴⁻.

The calculations were carried out by using a program package called JAMOL3 written by Kashiwagi et al.²⁰ So that the integral calculation could be made more tractable, an integral approximation scheme based on semiorthogonalized orbitals²¹ was utilized and the threshold value for the degree of overlap was set at 0.001. Open-shell calculations for the ground, ionized, and excited states have been performed in the restricted Hartree-Fock formalism as given by Roothaan.²² The corresponding vector coupling coefficients for various states were calculated according to ref 23. The electron-density maps were prepared by using the program called JAPIC1 written by Miyoshi et al.²⁴

Experimental Section

The photoelectron spectra were obtained from powdered samples mounted on a gold plate with a Jeol JESCA-3A electron spectrometer. The Mg K α X-ray line (1253.6 eV) was used for photoelectron

**Figure 1.** Valence shell spectra of XPS and Δ SCF orbital energies for $K_4[Fe(CN)_6]$.

excitation, and the measurements were carried out at a vacuum of 5×10^{-7} torr or below. Core-level spectra were recorded in regions of interest. The differences of two binding energies were obtained by synchronous measurements, which in most cases gave the values reproducible to ± 0.1 eV for the binding-energy differences. The valence spectra were measured for $K_4[Fe(CN)_6]$.

Results and Discussion

Cyanide Orbitals. The electronic structure of the free cyanide ion will be briefly discussed; the detail has been described in a previous report.¹⁵ The order of orbital levels is $3\sigma \ll 4\sigma < 1\pi < 5\sigma$. The 5σ MO strongly interacts with metal orbitals to result in the ligand-to-metal σ -electron donation; the 4σ , 1π , and 2π MO's also participate in the metal-ligand bonding to some extent.

Ionization Energies. The calculated orbital energies will be discussed in this section. Table I shows the observed N 1s and C 1s core orbital energies and the differences between them, $\Delta E(N\ 1s-C\ 1s)$. The results of DV- $X\alpha$ MO calculations¹⁶ and XPS experiments⁸ are also presented in Table I. The experimental binding energies from XPS are influenced by two effects, the charging of the insulator sample and the Madelung potential from surrounding ions. These effects are, however, nearly canceled in the binding-energy difference, $\Delta E(N\ 1s-C\ 1s)$,⁸ and thus a proper comparison can be made between the experimental and calculated values of $\Delta E(N\ 1s-C\ 1s)$. The values of $\Delta E(N\ 1s-C\ 1s)$ calculated by an ab initio MO method are about 4 eV larger than the experimental values. This may result from the neglect of the electron-correlation energies and the energy for the electron reorganization on ionization. If these energies remain constant among cyanide complexes, then the tendency of the calculated $\Delta E(N\ 1s-C\ 1s)$ values can be compared with that of experimental results. Thus the $\Delta E(N\ 1s-C\ 1s)$ values decrease from Cr³⁺ to Co³⁺ (117.5–117.3 eV) and from Fe³⁺ to Fe²⁺ (117.4–117.2), in agreement with the tendencies observed in the XPS results. The DV- $X\alpha$ MO results also showed similar tendencies. The differences in the calculated values of $\Delta E(Fe\ 2p-N\ 1s)$ and $\Delta E(Fe\ 2p-C\ 1s)$ between the Fe³⁺ and Fe²⁺ complexes are larger than those in the XPS values. This may indicate that the energy of electron reorganization is greater for Fe 2p than for N 1s or C 1s and that it is greater for Fe³⁺ than for Fe²⁺.

For valence shell ionization energies, the breakdown of Koopmans' theorem has been previously shown on the d-orbital ionization of [Co(CN)₆]³⁻, in which a significant relaxation takes place.¹⁵ On the other hand, Koopmans' theorem holds on the ionization of a ligand orbital.

The calculated orbital energies and orbital natures are shown in Table II for all the complexes examined. The positive orbital energies for some MO's of [Fe(CN)₆]⁴⁻ result from the neglect of the Madelung effect.²⁵ The order of valence shell energies

- (17) B. Roos, A. Veillard, and G. Vinot, *Theor. Chim. Acta*, **20**, 1 (1971).
 (18) T. H. Dunning, Jr., *J. Chem. Phys.*, **53**, 2823 (1970).
 (19) S. Jagner, *Acta Chem. Scand., Ser. A* **A29**, 255 (1975).
 (20) H. Kashiwagi, T. Takada, E. Miyoshi, and S. Obara, "Program JAMOL3", Program Library, Institute for Molecular Science Computer Center.
 (21) H. Kashiwagi and F. Sasaki, *Int. J. Quantum Chem., Symp.*, **7**, 545 (1973); H. Kashiwagi, *Int. J. Quantum Chem.*, **10**, 135 (1976).
 (22) C. C. J. Roothaan, *Rev. Mod. Phys.*, **32**, 179 (1960).
 (23) H. Kamimura, S. Sugano, and Y. Tanabe, "Ligand Field Theory and Its Applications", 4th ed., Shokabo, Tokyo, 1975.
 (24) E. Miyoshi, M. Sano, C. Watanabe, and H. Kashiwagi, "Program JAPIC1", Program Library, Institute for Molecular Science.

- (25) M. Sano and H. Yamatera, *Chem. Lett.*, 789 (1979).

Table II. Valence Shell MO Natures and Energies

symmetry	[Cr(CN) ₆] ³⁻		[Mn(CN) ₆] ³⁻		[Fe(CN) ₆] ³⁻		[Co(CN) ₆] ³⁻		[Fe(CN) ₆] ⁴⁻	
	energy	orbital nature	energy	orbital nature	energy	orbital nature	energy	orbital nature	energy	orbital nature
8t _{1u}	-0.053	π	-0.044	π	-0.038	π	-0.030	π	0.135	π
1t _{1g}	-0.058	π	-0.049	π	-0.044	π	-0.034	π	0.126	π
1t _{2u}	-0.071	π	-0.064	π	-0.060	π	-0.053	π	0.110	π
2t _{2g}	-0.096	π	-0.095	π	-0.096	π	-0.069	π	0.169	d
5e _g	-0.103	σ	-0.104	σ	-0.103	σ	-0.105	σ	0.092	σ
7t _{1u}	-0.115	σ	-0.114	σ	-0.113	σ	-0.112	σ	0.058	σ
8a _{1g}	-0.145	σ	-0.141	σ	-0.139	σ	-0.139	σ	0.026	σ
1t _{2g}	-0.195	d	-0.177	d	-0.194	d	-0.252	d	0.049	π
4e _g	-0.204	σ	-0.204	σ	-0.201	σ	-0.204	σ	-0.030	σ
6t _{1u}	-0.211	σ	-0.212	σ	-0.214	σ	-0.220	σ	-0.047	σ
7a _{1g}	-0.294	σ	-0.311	σ	-0.325	σ	-0.350	σ	-0.144	σ
6a _{1g}	-0.844	σ	-0.836	σ	-0.833	σ	-0.825	σ	-0.655	σ
3e _g	-0.835	σ	-0.828	σ	-0.823	σ	-0.813	σ	-0.645	σ
5t _{1u}	-0.836	σ	-0.828	σ	-0.824	σ	-0.815	σ	-0.646	σ

Table III. Computed Ionization Energies of [Fe(CN)₆]⁴⁻

species	orbital ^d	state	energy ^a	computed IP ^b	
				[Fe(CN) ₆] ⁴⁻	[Co(CN) ₆] ^{3-c}
[Fe(CN) ₆] ⁴⁻	¹ A _{1g}		-1815.0936		
[Fe(CN) ₆] ³⁻	2t _{2g}	² T _{2g}	-1815.4676	-10.18	-1.91 (1t _{2g})
	8t _{1u}	² T _{1u}	-1815.2453	-4.13	0.63
	1t _{1g}	² T _{1g}	-1815.2313	-3.75	0.65
	5e _g	² E _g	-1815.2258	-3.60	1.80
	1t _{2u}	² T _{2u}	-1815.2148	-3.30	1.12
	8a _{1g}	² A _{1g}	-1815.1303	-1.00	3.32

^a Values in au. ^b IP (eV) values are computed as the difference between the energy values of the ionized and ground states.

^c Reference 11. ^d Orbital shown is that from which an electron is removed.

for trivalent complexes is the same as that previously reported for [Co(CN)₆]³⁻, i.e., 4σ < dπ < 5σ < 1π. The metal dπ orbital is not the highest occupied MO (HOMO), but it lies below ligand orbitals. On the other hand, the order in the Fe²⁺ complex is 4σ < 5σ < 1π < dπ, the metal dπ being the HOMO. However, these orders may not correspond to those of ionization energies, because of the breakdown of Koopmans' theorem. The ionization potentials for the 8a_{1g}, 5e_g, 1t_{1g}, 1t_{2g}, 8t_{1u}, and 1t_{2u} MO's were obtained as the difference between

the SCF energies of the hole states and the ground state (ΔSCF). They are shown in Table III.

In the Fe²⁺ complex, the 2t_{2g} MO with the main component of the metal d orbital are most easily ionized with a large relaxation. The calculations as described above result in the decreasing order of orbital energies

$$3d\pi > \pi > \sigma$$

This is similar to the order previously reported for [Co(CN)₆]³⁻.¹⁵ Figure 1 shows the comparison of the calculated ΔSCF results with the observed valence-region XPS for K₄[Fe(CN)₆]. For an easy comparison, the position of the calculated energy level of dπ is arbitrarily taken as the reference to be fitted to the corresponding XPS peak in Figure 1. The relative positions of the calculated ΔSCF energy levels show a reasonable correlation with the XPS peaks. It is concluded that the ΔSCF results can be used for the assignment of the peaks of valence XPS.

Population Analysis. The results of the Mulliken population analysis are given in Tables IV and V. The charges of trivalent metals in the cyanide complexes are 1.74+ (Cr³⁺)–1.63+ (Co³⁺), and the iron charge in [Fe(CN)₆]⁴⁻ is 1.38+. These values differ from the DV-Xα MO results¹⁶ (Cr³⁺, 1.21+; Mn³⁺, 1.13+; Fe³⁺, 0.98+; Co³⁺, 0.84+; Fe²⁺, 0.83+)

Table IV. Orbital Populations

	[Cr(CN) ₆] ³⁻	[Mn(CN) ₆] ³⁻	[Fe(CN) ₆] ³⁻	[Co(CN) ₆] ³⁻	[Fe(CN) ₆] ⁴⁻
Metal					
3dσ	0.806	0.887	0.962	1.047	0.628
3dπ	2.969	3.931	4.907	5.884	5.662
4s	0.252	0.226	0.224	0.226	0.193
4p	0.379	0.384	0.410	0.396	0.341
atomic charge	1.744+	1.721+	1.662+	1.630+	1.379+
Carbon					
2s	1.705	1.675	1.663	1.645	1.741
2pσ	1.126	1.161	1.146	1.132	1.143
2pπ	1.623	1.617	1.620	1.615	1.502
atomic charge	0.447–	0.447–	0.422–	0.384–	0.379–
Nitrogen					
2s	1.616	1.603	1.618	1.651	1.587
2pσ	1.336	1.332	1.324	1.315	1.351
2pπ	2.398	2.410	2.418	2.427	2.585
atomic charge	0.343–	0.340–	0.355–	0.387–	0.517–

Table V. Bond Overlap Populations

	[Cr(CN) ₆] ³⁻	[Mn(CN) ₆] ³⁻	[Fe(CN) ₆] ³⁻	[Co(CN) ₆] ³⁻	[Fe(CN) ₆] ⁴⁻
M–C	0.190	0.185	0.189	0.186	0.150
σ	0.182	0.168	0.171	0.168	0.106
π	0.008	0.017	0.018	0.018	0.044
C–N	1.716	1.757	1.727	1.677	1.616
σ	0.657	0.704	0.673	0.634	0.629
π	1.059	1.053	1.054	1.043	0.987

and also from the results of Kida et al.⁹ and Alexander et al.^{2b} It is not surprising that different methods gave different values, since the population analysis is to some extent artificial.²⁶ However, the comparison of a series of results from the calculations after the same method can be expected to show a correct tendency.

In trivalent complexes, the metal charges decrease from Cr^{3+} to Co^{3+} (1.74+ to 1.63+) with an increase in the atomic number. This decrease in the metal charge results from the increase in the σ donation, while the π back-donation slightly increases from Cr^{3+} (0.03e) to Co^{3+} (0.12e). The same tendency has also been found by Larsson¹¹ in his MS- $X\alpha$ calculation and by Sano et al.¹⁶ in their DV- $X\alpha$ calculation. The present calculation, however, gave smaller estimates for both σ donation and π back-donation than those from the DV- $X\alpha$ ¹⁶ and MS- $X\alpha$ ¹¹ calculations. (The latter two calculations differ from each other in the method used for the estimation of atomic charges.) The carbon charge increases (0.45- to 0.38-), and the nitrogen charge decreases (0.34- to 0.39-) from Cr to Co. These tendencies are also consistent with our DV- $X\alpha$ results, although the DV- $X\alpha$ calculation gave less negative carbon charges (0.17- to 0.04-) and more negative nitrogen charges (0.53- to 0.60-).¹⁶

In the cyano complexes of Fe^{3+} and Fe^{2+} , the calculated metal charges are 1.662+ and 1.379+, respectively; the difference is much smaller than the difference in the oxidation number. The $3d\sigma$ population for Fe^{3+} (0.962) is greater than that for Fe^{2+} (0.628), while the difference between the formal number of $3d\pi$ electrons and the calculated population of the $3d\pi$ orbital is greater in the Fe^{2+} complex ($6.0 - 5.662 = 0.338$) than in the Fe^{3+} complex ($5.0 - 4.907 = 0.093$). This greater π back-donation in the Fe^{2+} complex, together with the greater σ donation to the $3d\sigma$, $4s$, and $4p$ orbitals in the Fe^{3+} complex, results in the small difference in the metal charge between the Fe^{2+} and the Fe^{3+} complex. The differences in the carbon and nitrogen charges also result mainly from the differences in the $2p\pi$ populations. The bond overlap populations (Table V) between metal and carbon are about 0.19 for trivalent complexes and 0.15 for $[\text{Fe}(\text{CN})_6]^{4-}$. This may indicate that the Fe-C bond is stronger in the Fe^{3+} than in the Fe^{2+} complex in accordance with the experimental findings.²⁷ However, the trend of the M^{3+} -C force constants is in contrast to that of the bond overlap populations.

Electron-Density Maps. More exact electron distribution in the cyano complexes can be given by the electron-density maps than by orbital populations. So that the change in charge distribution on the coordination of the CN^- ligands to a metal ion can be studied, the maps of the electron-density difference between the $[\text{M}(\text{CN})_6]^{(6-n)-}$ ion ($M = \text{Cr}^{3+}$, Co^{3+} , or Fe^{2+}) and the system of the M^{n+} ion plus six free CN^- ions are shown in Figure 2. The electron densities for the Cr^{3+} ion and for the Co^{3+} and Fe^{2+} ions were calculated as being of the electronic configurations of t_{2g}^3 and t_{2g}^6 in octahedral symmetry, respectively. The C-N bond lengths in the $(\text{CN})_6$ cluster were assumed to be the same as those in the complexes. The CN^- ions were placed along three axes ($x, y, z; -x, -y, -z$) with the same geometry as in their respective complex.

As can be seen from the increase in the electron density around the metal atom and the decrease around the ligands,

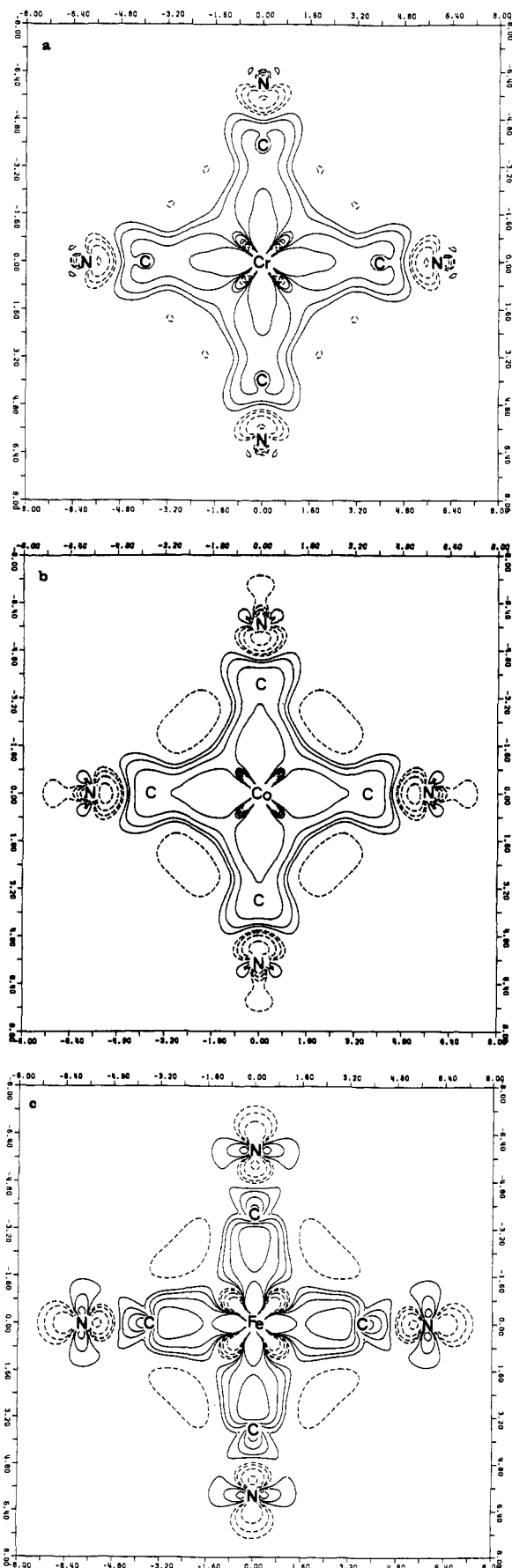


Figure 2. Electron-density differences between (a) $[\text{Cr}(\text{CN})_6]^{3-}$ and Cr^{3+} plus six free CN^- ions, (b) $[\text{Co}(\text{CN})_6]^{3-}$ and Co^{3+} plus six free CN^- ions, and (c) $[\text{Fe}(\text{CN})_6]^{4-}$ and Fe^{2+} plus six free CN^- ions. The first solid and dotted contours show $\pm 0.0025 \text{ e u}^{-3}$, and neighboring contours differ by a factor of 2.

(26) When a rigid spherical ion 4 Å in radius is introduced into a continuous medium with a dielectric constant of 78, then the free energy of solvation ($-\Delta G/\text{ion}$) will be 28.4, 16.0, and 7.1 eV for the ions with charges of 4-, 3-, and 2-, respectively; thus, a 4- ion, for example, is stabilized by 12.4 eV more as compared with a 3- ion. This suggests that $[\text{Co}(\text{CN})_6]^{3-}$ and $[\text{Fe}(\text{CN})_6]^{4-}$ can be stable in aqueous solution, and probably also in crystals, in spite of their instability (negative ionization energies) under vacuum. The negative values of the computed ionization potentials (IP) of the ions in vacuum should be overbalanced by the stabilization due to their electrostatic interactions with the surroundings.

(27) I. Nakagawa and T. Shimanouchi, *Spectrochim. Acta*, **18**, 101 (1962).

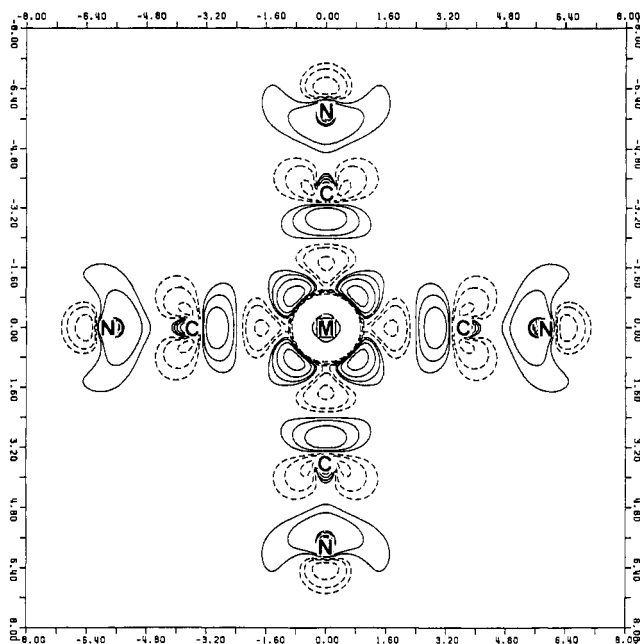


Figure 3. Electron-density difference between $[\text{Co}(\text{CN})_6]^{3-}$ and $[\text{Fe}(\text{CN})_6]^{4-}$. The first solid and dotted contours show $\pm 0.002 \text{ e au}^{-3}$, and neighboring contours differ by a factor of 2.

the electron flows from ligands into the metal. The shape of the positive region indicates the ligand-to-metal donation. The electron density in the cyanide ligands of the chromium complex decreases in the close vicinity of the carbon nucleus, increases in the outer region of the carbon atom, and decreases around the nitrogen nucleus. This shows that the cyanide ion is polarized by the positive charge of the metal ion and that the $2s$ population decreases and the $2p$ population increases in the carbon atom. The features in the Cr and Co complexes are very similar to each other; however, the increases of the metal $d\sigma$ and nitrogen $2p\pi$ electron densities are larger for the Co than for the Cr complex. This shows that the σ donation and π back-donation in the Co complex are larger than those in the Cr complex, in agreement with the increase in the nuclear charge and in the number of $d\pi$ electrons in going from Cr^{3+} to Co^{3+} . This is in agreement with Larsson's results¹¹ from $\text{MS-X}\alpha$ calculations and with our previous results¹⁶ from $\text{DV-X}\alpha$ calculations. Mulliken population analysis (Table IV) consistently shows the N $2p\pi$ electron densities are greater for the Co than for the Cr complex.

The decrease in the electron density of $d\pi$ and the increase in the N $2p\pi$ electron density are more pronounced in the Fe^{2+} complex than in the trivalent-metal complexes. This results from a larger π back-donation. In this connection, the map of electron-density difference between the isoelectronic $[\text{Fe}(\text{CN})_6]^{4-}$ and $[\text{Co}(\text{CN})_6]^{3-}$ is shown in Figure 3, in which $[\text{Fe}(\text{CN})_6]^{4-}$ was assumed to have the same geometry as that of $[\text{Co}(\text{CN})_6]^{3-}$. In going from the Co^{3+} to the Fe^{2+} complex, the electron density decreases in the metal $d\sigma$ orbital, while it decreases and increases in the metal inner and outer $d\pi$ regions, respectively. In the ligands, the electron density increases near the carbon nucleus, in the metal side of the carbon σ orbital, and in the nitrogen σ orbital, while it decreases in the carbon π orbital and increases in the nitrogen π orbital. The results of calculation can be elucidated as follows: as the nuclear charge of cobalt is larger than that of iron, the radical

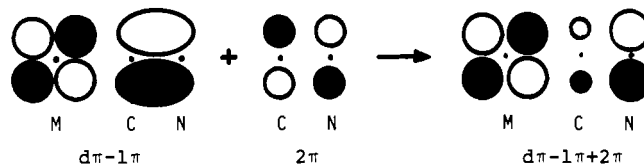


Figure 4. Orbital interaction of metal $d\pi$ and cyanide π orbitals of t_{2g} symmetry. The positive and negative signs of orbital wave functions are shown by white and black areas, respectively.

distribution of electrons in the metal orbital contracts and the ligands are polarized to a greater extent in the cobalt complex. This results in a higher electron density near the Co nucleus, a lower electron density in the outer region of the Co ion, and a higher electron density in the region of the metal $d\sigma$ orbital in the Co^{3+} complex than in the Fe^{2+} complex. This suggests that the $d\sigma$ density of Co^{3+} is higher than that of Fe^{2+} or that a larger fraction of the cyanide σ electron is transferred from each CN^- to Co^{3+} than to Fe^{2+} . The higher nitrogen $2p\pi$ and the lower carbon $2p\pi$ electron densities in the Fe^{2+} complex originate from a larger π back-donation; the π back-donation is the mixing of the CN^- 2π orbital with the MO of the $d\pi-1\pi$ type (an antiphase linear combination of the metal $d\pi$ and CN^- 1π orbitals) to result in the combination of the $d\pi-1\pi+2\pi$ type, in which 1π and 2π are of antiphase with respect to carbon $p\pi$ and of the same phase with respect to nitrogen $p\pi$. Then, a greater π back-donation weakens and strengthens the amplitudes on carbon and nitrogen respectively, as shown in Figure 3. The above discussion is schematically shown in Figure 4. Without the contribution of 2π , the $d\pi$ and 1π MO's would be formed of $d\pi+1\pi$ and $d\pi-1\pi$. The orbital energy levels of $[\text{Fe}(\text{CN})_6]^{4-}$ show the ordering of $1\pi < d\pi < 2\pi$, while the level order for trivalent-metal ions is $d\pi < 1\pi < 2\pi$. Then, the $d\pi-1\pi$ (or $1\pi-d\pi$) orbital is less stable than the $d\pi$ orbital for the Fe^{2+} complex and than the 1π orbital for the M^{3+} complexes. The energy separation between the $d\pi-1\pi$ (or $1\pi-d\pi$) and 2π orbitals is smaller for the Fe^{2+} than for the M^{3+} complexes, and therefore the mixing of 2π occurs to a greater extent in the Fe^{2+} complex. This explains the larger π back-donation in $[\text{Fe}(\text{CN})_6]^{4-}$.

Conclusions

The electronic structures of five octahedral cyanide complexes $[\text{M}(\text{CN})_6]^{3-}$ ($\text{M} = \text{Cr}, \text{Mn}, \text{Fe}, \text{and Co}$) and $[\text{Fe}(\text{CN})_6]^{4-}$, have been investigated by the LCAO MO SCF method of the Hartree-Fock type. The following important results were obtained. (1) The trend of the differences between the energies of the carbon and nitrogen core orbitals among the complexes is in good agreement with that of the XPS results. (2) The map of the electron-density difference between the complex ion and the system of independent metal and cyanide ions shows that both σ donation and π back-donation are larger for the Co^{3+} than for the Cr^{3+} complex. (3) A more extensive π back-donation is seen in the Fe^{2+} complex. These interactions are interpreted by the orbital-mixing rule.

Acknowledgment. The work was partly supported by the Joint Studies Program (1979-1980) of the Institute for Molecular Science. The computations reported in this paper have been carried out on the HITAC M-180 and M-200H computers of the Institute for Molecular Science.

Registry No. $[\text{Cr}(\text{CN})_6]^{3-}$, 14875-14-0; $[\text{Mn}(\text{CN})_6]^{3-}$, 14931-63-6; $[\text{Fe}(\text{CN})_6]^{3-}$, 13408-62-3; $[\text{Co}(\text{CN})_6]^{3-}$, 14897-04-2; $[\text{Fe}(\text{CN})_6]^{4-}$, 13408-63-4.